Optimization of Fractional-Order RLC Filters

Ahmed G. Radwan · M.E. Fouda

Abstract This paper introduces some generalized fundamentals for fractional-order $RL_\beta C_\alpha$ circuits as well as a gradient-based optimization technique in the frequency domain. One of the main advantages of the fractional-order design is that it increases the flexibility and degrees of freedom by means of the fractional parameters, which provide new fundamentals and can be used for better interpretation or best fit matching with experimental results. An analysis of the real and imaginary components, the magnitude and phase responses, and the sensitivity must be performed to obtain an optimal design. Also new fundamentals, which do not exist in conventional RLC circuits, are introduced. Using the gradient-based optimization technique with the extra degrees of freedom, several inverse problems in filter design are introduced. The concepts introduced in this paper have been verified by analytical, numerical, and PSpice simulations with different examples, showing a perfect matching.

Keywords Fractional calculus · Fractional filters · Optimization · RLC circuit · Sensitivity analysis · Fractional-order elements

1 Introduction

The history of fractional calculus dates back to 1695 with the work of scientists such as L'Hospital and Leibniz, but the first logic definitions were proposed by Liouville

A.G. Radwan (✉) · M.E. Fouda
Engineering Mathematics Department, Cairo University, 12613, Cairo, Egypt
e-mail: agradwan@ieee.org

M.E. Fouda
e-mail: m_elneanaei@ieee.org

A.G. Radwan
NISC Research Center, Nile University, Cairo, Egypt

in 1834, Riemann in 1847, and Grünwald in 1867 [21, 24]. Fractional calculus can be considered as a super set of integer-order calculus, which has the potential to accomplish what integer-order calculus cannot. The first approximation of the fractional-order derivative in terms of a complicated system of integer orders was proposed in 1964 [2], but this approximation is good only in a certain band of frequencies. Furthermore, different realizations of the fractional elements were introduced during the last few years [14, 15, 23, 25, 36, 38, 41] using different techniques. The theory of fractional-order elements comes from the frequency-dependent losses in the conventional elements as proved recently in [39, 42, 43]. Moreover, this theory was extended to the memristive elements (memristor, memcapacitor, and meminductor) [8, 26]. Many books and researches during the last three decades have aimed to increase the accessibility of fractional calculus for remodeling most of the existing applications and analyzing new models in basic natural sciences. For example, many papers recently have tried to model the electrical impedance of vegetables and fruits into simple electrical circuit connections using a single fractional capacitor [5, 12]. Generally, the fingerprints of the applied fractional calculus could be built up to include many physical phenomena based on differentiation and integration [37]. Various numerical techniques were introduced to solve linear and nonlinear fractional-order differential equations (FODEs) [3, 7] which model different physical problems.

Fractional calculus depends on the history of the function, which is more realistic and suitable for modeling, analyzing, and synthesizing and for solving many problems in bioengineering [17, 18]. Thus different biomedical models can be represented by simple connections of fractional circuit elements [22]. The existence of an extra degree of freedom enabled through choosing the fractional order makes its performance always superior to that of traditional integer calculus which can be used to describe the behavior of complex systems and materials. Moreover, modeling with fractional calculus is used to extract more generalized information and fundamentals [4, 6, 16, 19, 20]. In addition, the output can be optimized to be closer to the experimental results by adjusting the extra parameters and using a suitable optimization technique.

From the circuit perspective, the general theorems related to linear oscillators have been recently generalized to the fractional-order case, beginning with mathematical proofs, through circuit simulations, and ending with experimental results [28, 29]. A main basis in most of these generalizations is that the frequency of oscillation for using fractional elements of order α, is proportional to $\omega_{o1}^{1/\alpha}$ where ω_{o1} is the frequency of oscillation in the case of integer elements and if $\alpha = 0.5$ (order one-half), the oscillation frequency increases by a power of 2, which is required for many high frequency applications. Also, the generalizations of filter theorems are studied for one or two fractional elements of the same orders showing new fundamentals and features rather than those of known filters [30, 31, 40].

Due to the extra parameters in the fractional-order modeling over the conventional integer derivative, new responses and fundamentals and better approximations can be obtained using a suitable optimization technique. One of the major famous optimization criteria is gradient-based optimization, which is used to minimize a general function $F(x)$ from any starting point. This algorithm requires cycles of n iterations to be reset as the steepest descent direction that provides the best direction to minimize this

function. This optimization technique will be used to illustrate how fractional-order parameters can characterize filter responses which cannot be realized using integer-order filters.

In this paper, the generalized fractional impedance of all possible topologies for fractional-order basic circuits that use at most a resistor R, L_β (fractional inductor of order β), and a capacitor C_α (fractional capacitor of order α) are introduced, so this circuit has three traditional variables: R, L and C plus the two fractional orders α and β. This generalization is full of new fundamentals which cannot be obtained by the traditional elements, but where the generalized fractional impedance of the fractional-order $RL_\beta C_\alpha$ circuit can be used to model many phenomena in mechanical, biomedical, and even botanical systems. This paper discusses the frequency response behavior from different points of interest. The first point is the study of the basic analysis of the real and imaginary components, as well as the magnitude and phase responses. Many sensitivity analyses are introduced for different parameters. Second, the most important cases of this generalized impedance are studied when a real part (or phase) is zero (or $0, \pi$), an imaginary part (or phase) is zero (or $\pm\pi/2$), and finally when the magnitude equals zero; or the short circuit case. Finally, different optimization problems for designing filters are discussed based on the gradient-based optimization technique using the extra fractional-order parameters. Numerical and PSpice simulation results are also introduced with several examples. However, in order to discuss the previous characteristics, some fundamentals should be introduced.

1.1 Basic Definition of Fractional Capacitor

The most important definition of the fractional derivative is introduced by Caputo [24] which is denoted by Eq. (1). If $\alpha = 1.2$, then $m = 2$, so the fractional derivative of order 1.2 is equivalent to an integer derivative of order 2 followed by a fractional integral of order 0.8,

$$
{}_aD_t^\alpha f(t) := \begin{cases} \frac{1}{\Gamma(m-\alpha)} \int_a^t \frac{f^{(m)}(\tau)}{(t-\tau)^{\alpha+1-m}} \, d\tau & (m-1) < \alpha < m \\ \frac{d^m}{dt^m} f(t) & \alpha = m \end{cases} \tag{1}
$$

There are many numerical approximations for the above definition; the most important one is driven as in (2) by Grünwald-Letnikov [27]. In this definition Γ and h are the gamma function and the step size, respectively. It is clear that the summation takes into account all previous values of $f(t)$ which cover all the historical background of the function. When $\alpha = 1$, all items inside the summation will be zero except for $m = 0, 1$, which will be reduced to the traditional backward difference formula,

$$
{}_aD_t^\alpha f(t) = \lim_{h \to 0} \frac{1}{h^\alpha \Gamma(-\alpha)} \sum_{m=0}^{\frac{t-a}{h}} \frac{\Gamma(m-\alpha)}{m!} f(t-mh) \tag{2}
$$

Another advantage of the fractional derivative comes from the Laplace transform of the fractional derivative, for example, $L\{{}_aD_t^\alpha f(t)\} = F(s)/s^\alpha$, which is equivalent to the relation between the current and voltage across the fractional-order capacitor
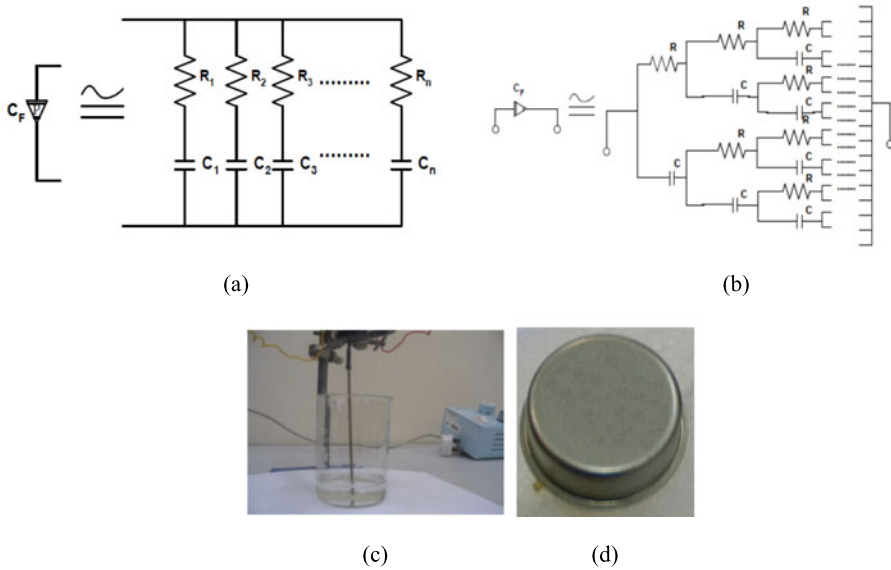
(a)   (b)

(c)   (d)

Fig. 1 Floating fractional-order capacitor realizations

$V(s) = I(s)/(C_f s^\alpha)$, where C_f is the value of the fractional capacitor. Then the phase difference between the current and voltage will be $\alpha\pi/2$. In the case of integer order of the capacitor ($\alpha = 1$), the general case returns to the well-known phase difference $\pi/2$.

1.2 Realization of Fractional Elements

The modeling of fractional-order systems (e.g., the fractional capacitor) was discussed during the previous three decades from different points of view. The mathematical approximation of the equivalent transfer function ($1/s^\alpha$) to higher integer order within a certain region of frequencies, passing through its realization using many branches of resistors and capacitors whose values are related to certain factors, where $0 < \alpha < 1$, is shown in Fig. 1(a) [41], or a tree shape of equal values can be used to realize the half-order fractional element as shown in Fig. 1(b) [9]. New realizations of fractional elements using chemical reactions between different materials are shown in Fig. 1(c) [1, 9, 13]. All these realizations are a good approximation for the fractional element within a certain range of frequencies. Moreover, a new half-order capacitor based on fractal structures was introduced in [10, 11].

In the near future, if scientists are able to realize a wide band fractional capacitor of order α where $0 < \alpha < 1$ only, this will be enough to obtain the full range of α as follows:

- A fractional capacitor of order $1 < \alpha \leq 2$ can be obtained through the use of a general impedance converter (GIC) whose input impedance is given by $Z_{in} = Z_1 Z_2 Z_3/(Z_4 Z_5)$.

- A fractional inductor of order $0 < \beta \leq 2$ can be realized by using the well-known gyrator circuit whose input impedance is inversely proportional to Z_L, so if Z_L is a fractional capacitor of order β, then the input impedance of the gyrator will be a fractional inductor of the same order.

1.3 Boundary Characteristic Frequencies

An analysis of the generalized impedance of $RL_\beta C_\alpha$ shows new fundamental frequencies [32–34] which do not exist in the conventional case. The definitions of these frequencies are as follows.

- *Pure real angular frequency* (ω_{pr}): the frequency at which the fractional impedance is pure real (the phase equals 0 or π). Then, if a sinusoidal voltage (or current) source is applied at this frequency, the current (or voltage) will have the same oscillation and fixed amplitude. This frequency exists if the circuit has at least two fractional-order elements.
- *Pure imaginary angular frequency* (ω_{pi}): the frequency at which the fractional impedance is pure imaginary (the phase equals $\pm \pi/2$). This frequency exists if the circuit has two elements at least, and at least one of them is of fractional order.
- *Short* (*or open*) *circuit angular frequency* (ω_{sc} *or* ω_{oc}): the frequency at which the magnitude equals zero. In this case, another necessary condition between the circuit elements should exist. Ideally, in this case, the current (or voltage) will show free oscillation with ω_{sc} and with a magnitude depending on the initial storage energy and circuit variables. This frequency will exist if the circuit has at least two fractional-order elements.

2 Fractional Impedance of Series $RL_\beta C_\alpha$ Circuit

The Laplace formula of the total impedance for the series connection of a conventional series RLC circuit is given by $Z(s) = R + sL + 1/(sC)$, where $s = j\omega$, $Z(s)$ will be divided into either real and imaginary parts, or magnitude and phase parts, which have the following fundamentals:

- The real part depends on R only; however, the imaginary part depends on $\{\omega, C, L\}$. Both the magnitude and phase responses are functions of $\{R, L, C, \omega\}$. Then there are two independent basic equations in four variables at maximum.
- The real part (related to the power loss) exists if and only if $R \neq 0$, and the imaginary part (related to the restoring energy) is depleted if and only if $\omega_c = 1/\sqrt{LC}$, which is the boundary frequency between inductive and capacitive equivalent impedance; so if $\omega > \omega_c$, the impedance will be inductive, and otherwise the impedance will be capacitive.
- The magnitude is always greater than zero, while the phase must always be inside the range $(-\pi/2, \pi/2)$.
- The magnitude response will be very large at both very low and very high frequencies; however, it has a critical minimum at ω_c, which is known as the resonance frequency.
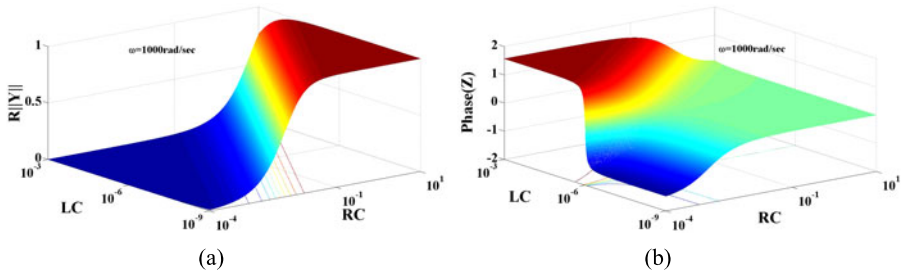
Fig. 2 The magnitude and phase of the admittance of the series RLC circuit at $\omega = 1000$ rad/sec

Fig. 3 (**a**) Simple fractional-order $RL_\beta C_\alpha$ circuit, (**b**) the corresponding phasor diagram of the fractional elements
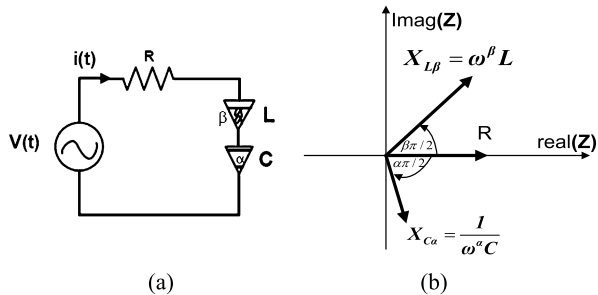

Figure 2(a) shows the ratio between the resistor R and the impedance magnitude $\|Z\|$, which is a function of only three variables $\{RC, LC, \text{ and } \omega\}$ at a specific value of $\omega = 1000$ rad/sec. The phase response at the same frequency is plotted in Fig. 2(b) where the phase changes its sign at $LC = 10^{-6}$, which is expected because the resonance frequency $\omega_c = 1000$ rad/sec.

The equivalent impedance of the simple fractional-order $RL_\beta C_\alpha$ circuit shown in Fig. 3(a) is given by (3), and the fractional phasor diagram is shown in Fig. 3(b). This phasor diagram describes the magnitude and phase of the impedance for each element in the circuit. Since the reactance of the fractional inductor makes an angle $\beta\pi/2$ with R, it can be resolved into two parts, one in the same direction of R which is proportional to $\cos(\beta\pi/2)$ and the other perpendicular to R with factor $\sin(\beta\pi/2)$. The same can be applied to the fractional capacitor.

$$\frac{Z(j\omega)}{R} = \left(1 + \frac{\cos(\frac{\alpha\pi}{2})}{\omega^\alpha RC} + \frac{\omega^\beta L \cos(\frac{\beta\pi}{2})}{R}\right) + j\left(-\frac{\sin(\frac{\alpha\pi}{2})}{\omega^\alpha RC} + \frac{\omega^\beta L \sin(\frac{\beta\pi}{2})}{R}\right) \quad (3)$$

The general impedance of $RL_\beta C_\alpha$ where $0 < \alpha, \beta < 2$ is more complicated, since instead of independent terms in both the real and imaginary parts, there will be dependent terms, as will be shown. In order to simplify the magnitude response, two variables (x and y) will be defined as follows:

$$x = \frac{1}{\omega^\alpha RC}, \qquad y = \frac{\omega^\beta L}{R} \quad (4a)$$

$$\frac{Z(j\omega)}{R} = \left(1 + x\cos\left(\frac{\alpha\pi}{2}\right) + y\cos\left(\frac{\beta\pi}{2}\right)\right)$$

$$+ j\left(-x\sin\left(\frac{\alpha\pi}{2}\right) + y\sin\left(\frac{\beta\pi}{2}\right)\right) \tag{4b}$$

Both the real and imaginary parts of the circuit impedance have an important role in design and analysis, such as power (power loss, power storage, power factor), especially for biomedical applications. The real part of the $RL_\beta C_\alpha$ circuit depends on four parameters, which are α, β, RC, and L/R. Any small changes in the fractional orders will introduce big differences in the real part; thus, they are the most sensitive parameters with respect to the real part. The fractional order α exists only in the second term of the real part T_{2r}, where $T_{2r}(\alpha, \omega) = \cos(\alpha\pi/2)/\omega^\alpha$.

3 New Fundamentals of the $RL_\beta C_\alpha$ Circuit

During the next study, three major special cases will be studied. The first case is when the magnitude response is pure real, which means the phase response has an angle of 0 or π. This case demonstrates the instant when all the power delivered to the circuit is converted into losses. The second special case is when the magnitude response is pure imaginary (phase response across the lines $\pm\pi/2$), which happens when all the delivered power to the circuit is stored inside without any kind of loss. The last, very special case studied is when both real and imaginary parts deplete the short circuit magnitude response. In this case, the circuit would not store or lose any kind of incoming power, and if the circuit is closed, any already-stored power will circulate and freely oscillate.

3.1 Pure Resistive

In this case $Z(j\omega)$ is pure real (lossy element). As shown from (3), the imaginary part will be zero if the operating frequency satisfies (5a), and then the impedance can be simplified as shown in (5b) which is highly dependent on all parameters. When $\omega > \omega_{pr}$, the generalized impedance in (3) will be an inductive impedance, but when $\omega < \omega_{pr}$, the generalized impedance will be a capacitive impedance. When α or $\beta = 2$ (the fractional element in this case will act as a frequency-dependent negative resistor (FDNR)), the general impedance in (3) will always have an imaginary part, but if both of them are equal to 2, the general impedance will only be a real part (without any constraint on ω); however, this real part will be frequency dependent. Also, if $\alpha = \beta$ the pure resistive frequency will be $\omega_{pr} = (LC)^{-1/(2\alpha)}$ for $\alpha \neq 2$, and the corresponding pure real impedance $Z(j\omega_{pr}) = R + 2\sqrt{L/C}\cos(\frac{\alpha\pi}{2})$. For the integer case, when $\alpha = \beta = 1$, the pure resistive frequency will be $\omega_{pr} = 1/\sqrt{LC}$, which is known as the resonance frequency, while the pure real impedance $Z(j\omega_{pr}) = R$.

$$\omega_{pr} = \left(\frac{\sin(\frac{\alpha\pi}{2})}{LC\sin(\frac{\beta\pi}{2})}\right)^{\frac{1}{\alpha+\beta}}, \quad \alpha, \beta \neq 2 \tag{5a}$$
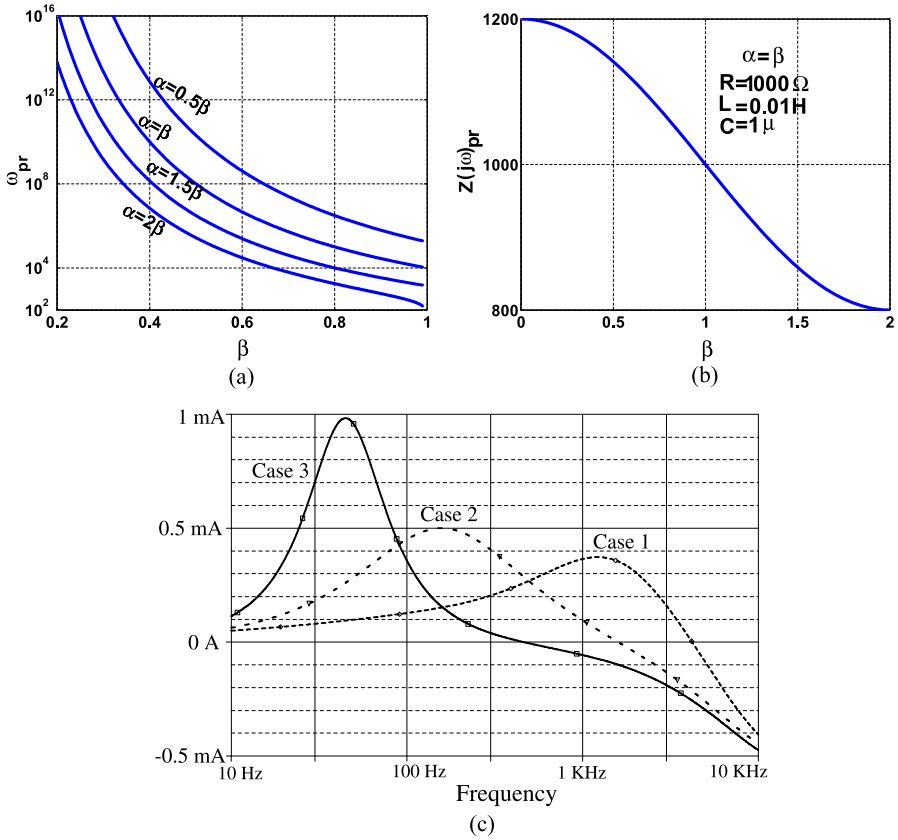
Fig. 4 (**a**) The relation between ω_{pr} and β for different cases, (**b**) the pure real impedance $Z(j\omega)_{\mathrm{pr}}$ for $\alpha = \beta$, (**c**) the imaginary part of the current versus frequency for three different cases

$$Z(j\omega_{\mathrm{pr}}) = R + \sin\left(\frac{(\alpha+\beta)\pi}{2}\right)\left(\frac{L^{\alpha}}{C^{\beta}\sin^{\alpha}(\frac{\alpha\pi}{2})\sin^{\beta}(\frac{\beta\pi}{2})}\right)^{\frac{1}{\alpha+\beta}} \tag{5b}$$

Figure 4(a) shows a relation between the pure resistive frequency and the fractional order β. This frequency has a very wide range according to the relation between α and β. Figure 4(b) shows the input impedance magnitude $\|Z(j\omega)\|$ at pure resistive frequency ω_{pr} for different β; it is clear that when $\beta = 1$, the real part of $Z(j\omega) = \|Z(j\omega)\| = R$. Also $Z(j\omega)$ will be restricted to the values from 800 Ω to 1200 Ω. Figure 4(c) shows the PSpice simulation results of the imaginary part for the current passing through the $RL_{\beta}C_{\alpha}$ circuit versus frequency in three different cases. It is clear that each curve will cross the horizontal line $i = 0$ A (that means no imaginary part, or its impedance is pure real) at the same calculated frequency ω_{pr} from (5a) which is $L = 0.01$ and $R = 1$ kΩ for three different cases: the first case at $\alpha = 0.5$, $C = 10$ μ, the second case at $\alpha = 1$, $C = 1$ μ, and the last case at $\alpha = 1.4$, $C = 0.371$ μ.
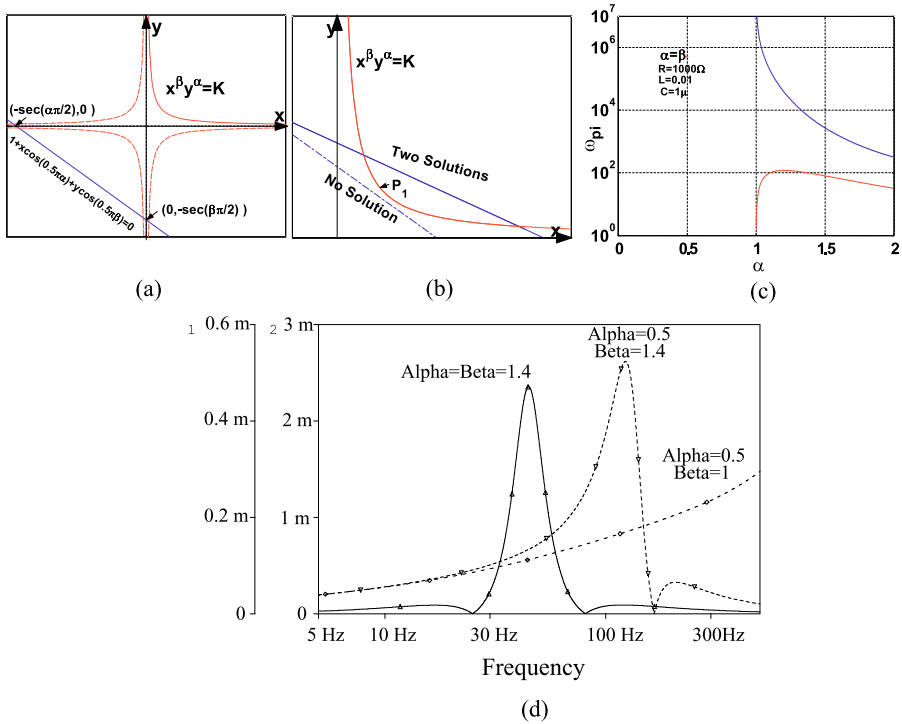
Fig. 5 (**a**) The relation between x and y for the first case, (**b**) the relation between x and y for the third case, (**c**) pure imaginary frequency versus α in the case of $\alpha = \beta$, (**d**) the real part of the current when $R = 1, 6\,\text{k}\Omega$, and for different cases

3.2 Pure Inductive or Capacitive

In the second alternative $Z(j\omega)$ is pure imaginary (lossless, or storing element). The condition for (3) to be real-free is given by (6a), but this equation is nonlinear for ω and depends on five independent variables L, C, R, α, and β.

$$\omega^{\alpha+\beta} LC \cos\left(\frac{\beta\pi}{2}\right) + \omega^{\alpha} RC + \cos\left(\frac{\alpha\pi}{2}\right) = 0 \tag{6a}$$

$$1 + x \cos\left(\frac{\alpha\pi}{2}\right) + y \cos\left(\frac{\beta\pi}{2}\right) = 0 \tag{6b}$$

To study different solutions for this equation, let's use the two definitions in (4a); then the equivalent equation will be (6b). Also, by removing ω from both definitions (4a), the following relation will be obtained:

$$x^{\beta} y^{\alpha} = \frac{L^{\alpha}}{C^{\beta} R^{\alpha+\beta}} = K \tag{6c}$$

Equation (6b) represents a straight line with slope $m = -\sec(\beta\pi/2)\cos(\alpha\pi/2)$ as shown in Fig. 5(a), with axis intersections at $(0, -\sec(\beta\pi/2))$, and $(-\sec(\alpha\pi/2), 0)$;

however, Eq. (6c) represents two curves from the four illustrated in Fig. 5(a), where the solid curve (located in the first quadrant) must be one of the two curves, and the curvature of these lines is controlled by the variables (α, β, K). The intersection(s) between the two equations is (are) the solution(s) of the previous equation. Then if x or y is given, the frequency ω will easily be obtained from (6b). Since x and y must be positive values for acceptable solutions, the solid curve is our main interest. This conclusion will lead to three general cases:

1. $\alpha, \beta < 1$: The intersection point has a negative value, which is unacceptable as a result, thus no solution (the impedance must have real part), as shown in Fig. 5(a).
2. $\alpha < 1 < \beta$ or $1 < \alpha$: The line makes an angle less than 45°; the system has a unique solution for (x, y), which means single or multiple operating frequencies depending on the value of $(\alpha + \beta)$.
3. $\alpha, \beta > 1$: The line makes an angle greater than 45° and part of it is inside the first quadrant. In this case, there are two possibilities according to the line intersecting the solid curve or not, as shown in Fig. 5(b). The critical value between the two possibilities is the point p_1 and is given by

$$P_1 = \left(\left(K r^\alpha \right)^{\frac{1}{\alpha+\beta}}, \left(k r^{-\beta} \right)^{\frac{1}{\alpha+\beta}} \right) \tag{7}$$

where $r = \beta \cos(\beta\pi/2)/(\alpha \cos(\alpha\pi/2))$. p_1 is the point on the solid curve having the same slope m. The two possibilities can be described as follows.
   (a) If P_1 lies below the line, there is no intersection, and no solution.
   (b) If P_1 lies above the line, there are two different intersections, and many operating frequencies.

In the special case when $\alpha = \beta$, Eq. (6a)–(6c) can be solved by quadratic form and is given by (8). The magnitude under the square root is always less than 1. Since the solutions must be positive and in this case there are two different solutions, Fig. 5(c) shows these two possible values of ω_{pi} versus α. For the well-known study of the resonance circuit of integer order, there is no definition about pure imaginary impedance because (8) has no solution when $\alpha = \beta = 1$. PSpice simulation results for three different cases which are equivalent to the previously discussed cases are shown in Fig. 5(d), where case 1 represents no solution for $\alpha = 0.5$, $\beta = 1$, $C = 10$ μ, and $L = 0.01$, case 2 has one solution at $f_{pi} \approx 167$ Hz for $\alpha = 0.5$, $\beta = 1.4$, $C = 10$ μ, and $L = 0.371$, and case 3 has two different solutions at $f_{pi1} \approx 25$ Hz; and $f_{pi2} \approx 81.2$ Hz for $\alpha = \beta = 1.4$, $C = 0.371$ μ, and $L = 0.371$. All the previous values are the same as given by the solution of (6a)–(6c).

$$\omega_{pi} = \left(\frac{R}{2L \cos(\frac{\alpha\pi}{2})} \left(-1 + \sqrt{1 - \frac{4L}{R^2 C} \cos^2 \left(\frac{\alpha\pi}{2} \right)} \right) \right)^{\frac{1}{\alpha}} \tag{8}$$

3.3 Short Circuit Impedance

It is well known from our previous study that the RLC circuit will not oscillate freely as a self-oscillation circuit. But this will be different in the generalized fractional-order $RL_\beta C_\alpha$ circuit which can oscillate without any source (just short circuit).
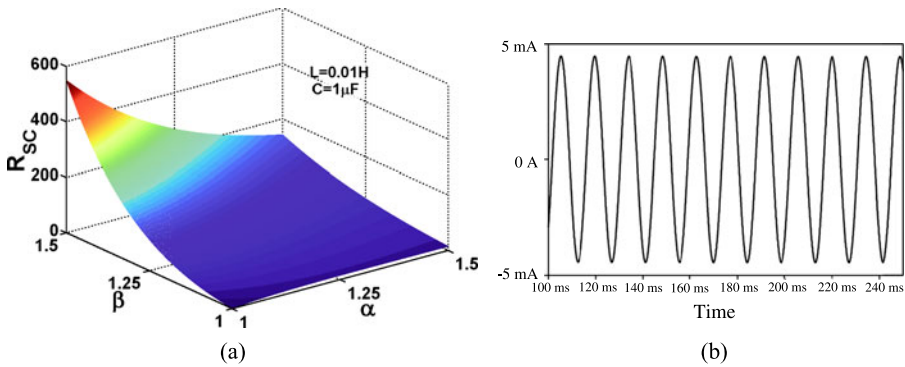
Fig. 6 (a) The short circuit resistance for different values of α and β, (b) PSpice transient response for free oscillation of $RL_\alpha C_\beta$ for $R = 137\ \Omega$, $\alpha = 1.4$, $\beta = 1$, $C = 0.371\ \mu$, and $L = 1$

A nonautonomous linear oscillator can oscillate freely if and only if its equivalent impedance is a short circuit (zero loss, and zero storing energy). Then if both the real and imaginary parts of (3) are forced to be zero, the frequency of oscillation will be obtained as $\omega_{\mathrm{osc}} = \omega_{\mathrm{pr}}$, and the condition of oscillation will be given by (9). The short circuit resistance is illustrated for different values of α and β in Fig. 6(a). For $\alpha, \beta \leq 2$, this condition will not be satisfied unless $(\alpha + \beta) > 2$. This explains why in integer-order systems, the RLC circuit cannot oscillate. When $\alpha = 1.4$, $C = 0.371\ \mu$, $\beta = 1$, and $L = 1$, the value of $R_{\mathrm{SC}} \approx 317.9\ \Omega$, and $\omega_{\mathrm{osc}} \approx 473.6$ rad/sec. PSpice simulation results of the current passing through this $RL_\beta C_\alpha$ circuit without any voltage source, but with initial resistance given by Eq. (9), are shown in Fig. 6(b).

$$R_{\mathrm{sc}} = -\sin\left(\frac{(\alpha + \beta)\pi}{2}\right)\left(\frac{L^\alpha}{C^\beta \sin^\alpha(\frac{\alpha\pi}{2})\sin^\beta(\frac{\beta\pi}{2})}\right)^{\frac{1}{\alpha+\beta}} \tag{9}$$

4 Gradient-Based Optimization of the $RL_\beta C_\alpha$ Filters

The gradient-based optimization requires calculating the error function as well as the derivatives in each iteration to simplify the search direction, which provides better convergence than other techniques and is preferable in many inverse problems such as cancer detection as presented in [35]. Therefore, the study of the sensitivity analysis is essential before starting this type of optimization. In this paper, the function fminimax from the optimization toolbox of the Matlab program is selected to perform the optimization technique. The next two subsections will discuss the sensitivity analysis of the fractional-order RLC circuit with respect to all possible design parameters. Finally, the last subsection will introduce different optimization examples for different orders.
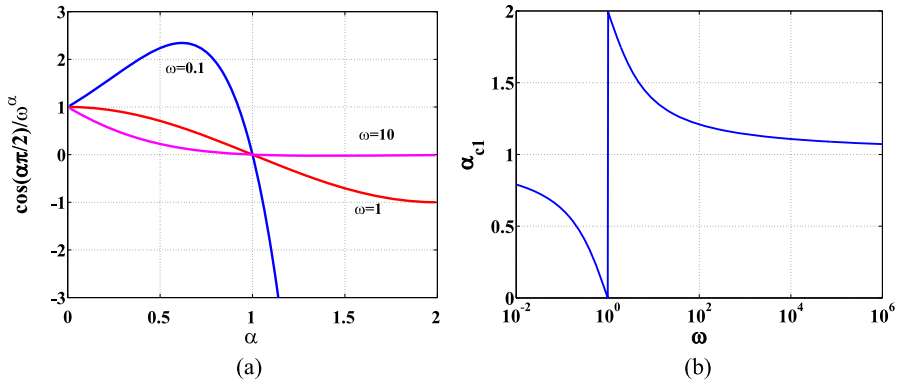
Fig. 7 (a) T_{2r} versus α for different frequencies, (b) α_{c1} versus frequency ω

4.1 Sensitivity Analysis of the Real and Imaginary Parts

The sensitivity of the second term of the real part T_{2r} with respect to α is given by

$$\frac{\partial T_{2r}}{\partial \alpha} = -\frac{(\frac{\pi}{2})\sin(\frac{\alpha\pi}{2}) + \ln(\omega)\cos(\frac{\alpha\pi}{2})}{\omega^\alpha} \tag{10}$$

$\partial T_{2r}/\partial \alpha$ is almost negative. The critical values of this term can be obtained as given in (11). Then if $\omega = \{0.1, 10, 10^3, 10^5\}$, and the corresponding critical values $\alpha_{c1} = \{0.6189, 1.3811, 1.1423, 1.0721\}$,

$$\left.\frac{\partial T_{2r}}{\partial \alpha}\right|_{\alpha=\alpha_{c1}} = 0 \quad \rightarrow \quad \alpha_{c1} = \begin{cases} 2 - \frac{2}{\pi}\tan^{-1}(\frac{2}{\pi}\ln(\omega)) & \omega > 1 \\ \frac{2}{\pi}\tan^{-1}(\frac{-2}{\pi}\ln(\omega)) & \omega < 1 \end{cases} \tag{11}$$

Traditionally, when $\alpha = 1$, the term T_{2r} disappears; however, for any other non-integer order the ratio between the added term and the traditional term is $T_{2r}/(RC)$, which means that any small values of T_{2r} will be amplified by the ratio $(1/(RC))$ which is in the order of thousands. Then the study of T_{2r} is not optional, as shown in the following figures. Figure 7(a) shows the sketch of the second term T_{2r} versus the fractional order α. The maximum value of T_{2r} increases as the operating angular frequency is less than one, and these maximum values may increase to higher than 2, which effectively means that the traditional term is neglected with respect to the added term. As ω increases, the effect of the added term decreases and tends to zero at very high frequencies. Also, when α is very small, then T_2 tends to one; however, when $\alpha > 1$, the added term becomes negative. This lets us explore the possibility of the following fact for the series RC_α circuit. The real part of the equivalent impedance is always greater than R when $\alpha < 1$ and equal to R at $\alpha = 1$. But, when $\alpha > 1$, the real part may be positive, zero, or negative according to the operating frequency and RC value at any fractional order α. This specific frequency is called the pure real angular frequency ω_{pr}. Figure 7(b) shows the relationship between the critical value α_{c1} versus ω, which shows a decreasing function in the whole domain. The graph
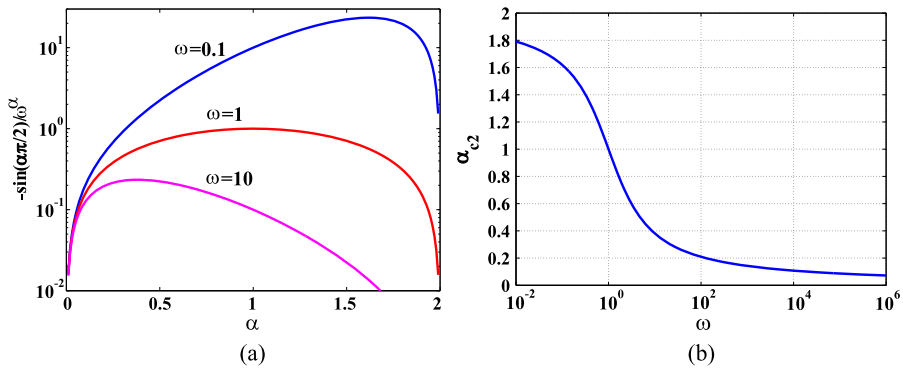
Fig. 8 (a) T_{1i} versus α for different frequencies ω, (b) α_{c2} versus frequency ω

splits into two independent curves at $\omega = 1$, and as ω tends to ∞ the critical α_{c1} tends to 1.

Note that $\alpha_{c1}|_\omega + \alpha_{c1}|_{1/\omega} = 2$, which means that the addition of the two critical fractional powers at any frequency and its reciprocal is 2. Also, the ratio between their magnitudes is $T_{2r}(\alpha_{c1}, 1/\omega)/T_{2r}(2 - \alpha_{c1}, \omega) = -\omega^2$. The negative sign in this ratio means that one of them is maximum and the other is minimum. For low frequencies which are less than one and where $\alpha_{c1} < 1$, T_{2r} will be maximum; the opposite of this occurs for frequencies greater than one. As shown in Fig. 8(a), for $\omega = 0.1$ rad/sec, and $\omega = 10$ rad/sec the magnitude ratio between their extremes is 200, maximum with a big value for the first and minimum with a small magnitude in the second.

Similarly, the effect of the fractional order α on the imaginary part can be discussed. The imaginary part of the equivalent impedance is composed of two independent parts; the first is concerned with the fractional-order α with RC, and the second is related to β with L/R values. The first term is $T_{1i}(\alpha, \omega, RC) = \sin(\alpha\pi/2)/\omega^\alpha$, and its derivative with respect to the fractional order α is given as $(\partial T_{1i})/\partial\alpha = ((\pi/2)\cos(\alpha\pi/2) - \ln(\omega)\sin(\alpha\pi/2))/\omega^\alpha$. So, the critical order of the imaginary part is given by

$$\left.\frac{\partial T_{1i}}{\partial\alpha}\right|_{\alpha=\alpha_{c2}} = 0 \quad \rightarrow \quad \alpha_{c2} = \begin{cases} \frac{2}{\pi}\cot^{-1}(\frac{2}{\pi}\ln(\omega)) & \omega \geq 1 \\ 2 + \frac{2}{\pi}\cot^{-1}(\frac{2}{\pi}\ln(\omega)) & \omega < 1 \end{cases} \tag{12}$$

From the previous discussion regarding the effect of the fractional-order α, there is a relationship between both critical orders α_{c1} and α_{c2} as follows: $\alpha_{c1} = \alpha_{c2} + \text{sgn}(\omega - 1)$, where $\text{sgn}(.)$ is the sign function which produces either 1 or -1. Figure 8(a) shows the first term T_{1i} in the imaginary part of the equivalent impedance versus α for different values of ω. The critical fractional order α_{c2} versus ω is shown in Fig. 8(b).

$$\frac{\|Z(j\omega)\|}{R} = \sqrt{1 + x^2 + y^2 + 2xy\cos\left(\frac{\alpha+\beta}{2}\right) + 2x\cos\left(\frac{\alpha\pi}{2}\right) + 2y\cos\left(\frac{\beta\pi}{2}\right)} \tag{13}$$
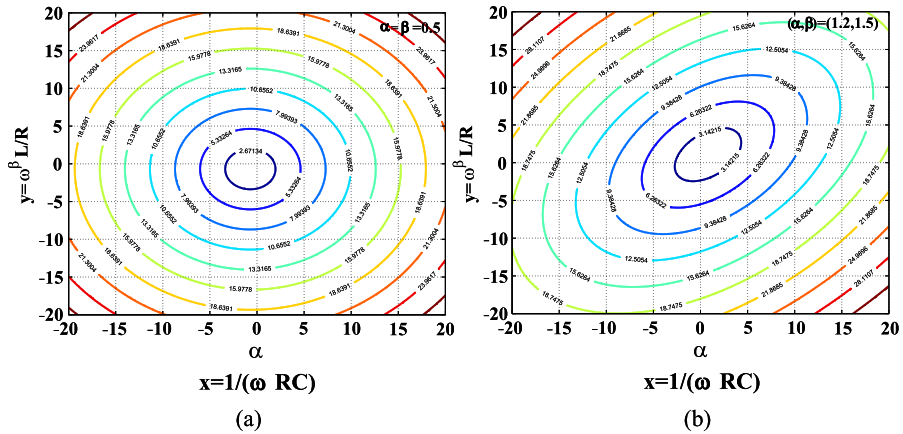
Fig. 9 Contours of $\|Z\|/R$ for (**a**) $\alpha, \beta < 1$, (**b**) $\alpha, \beta > 1$

As known, the impedance magnitude is always positive, but it is very interesting to study the location where there is zero magnitude. According to (13), the 3D graph of the magnitude as a function of x and y is paraboloid; the contours for this magnitude function are shown in Fig. 9 for two different cases. When $\alpha = \beta = 0.5$, the contours which have constant magnitude values are circular as shown in Fig. 9(a), but the center of all these circles exists in the third quarter $(x, y < 0)$, which is unacceptable since both x and y are always positive. This center is the location for zero magnitude. However, when $\alpha, \beta > 1$, the contours are ellipses and the center of these ellipses lies in the first quadrant as shown in Fig. 9(b).

Figure 10 shows the effect of the magnitude response with respect to the fractional orders α and β at certain values of the other parameters, ω, RC, and LC. When $\omega = 1$ Mrad/sec, $RC = 0.001$, and $LC = 10^{-8}$, Fig. 10(b) shows $R\|Y(\alpha, \beta)\|$ versus the full ranges of both fractional orders, which have a wide range for different orders. The effect of decreasing ω is clear from Fig. 10(a, b), where the original surface has been shifted in both directions and the y-axis is limited to 0.1 when $\omega = 10$ rad/sec. The effect of increasing LC is shown in Fig. 10(a, c), where the surface has been shifted mainly to the back. However, the increase of RC is shown in Fig. 10(a, d).

The phase of the equivalent impedance of the series $RL_\beta C_\alpha$ can be defined by (14), and the surface of this phase as a function of the fractional orders is shown in Fig. 11(a) at $\omega = 1$ Mrad/sec, $RC = 0.001$, and $LC = 10^{-8}$. Then for fixed circuit parameters and at a specific angular frequency, the phase changes from negative values to π. To verify the concept that this series circuit can oscillate freely, let us study the admittance value at $\omega = 1000$ rad/sec, $RC = 0.001$, and $LC = 10^{-8}$ as shown in Fig. 11(b), where there is a discontinuity at certain points in the domain (α, β). The phase response of the impedance is shown in Fig. 11(c), which shows some regions of complex discontinuities. To clarify this region, Fig. 11(d) illustrates the contours of this phase surface, where the point of interest is very clear.

$$\angle Z(j\omega) = \tan^{-1}\left(\frac{y\sin(\frac{\beta\pi}{2}) - x\sin(\frac{\alpha\pi}{2})}{1 + y\cos(\frac{\beta\pi}{2}) + x\cos(\frac{\alpha\pi}{2})}\right) \qquad (14)$$
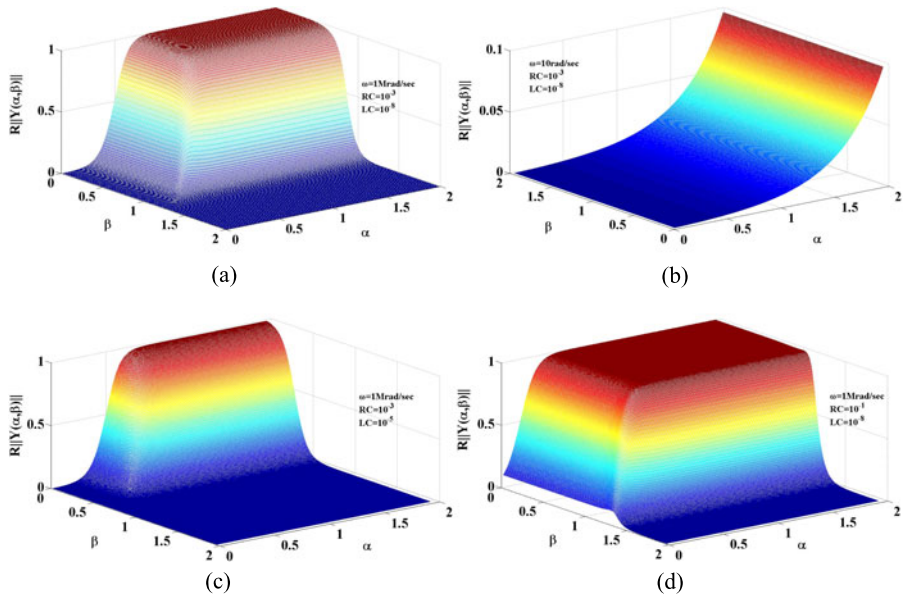
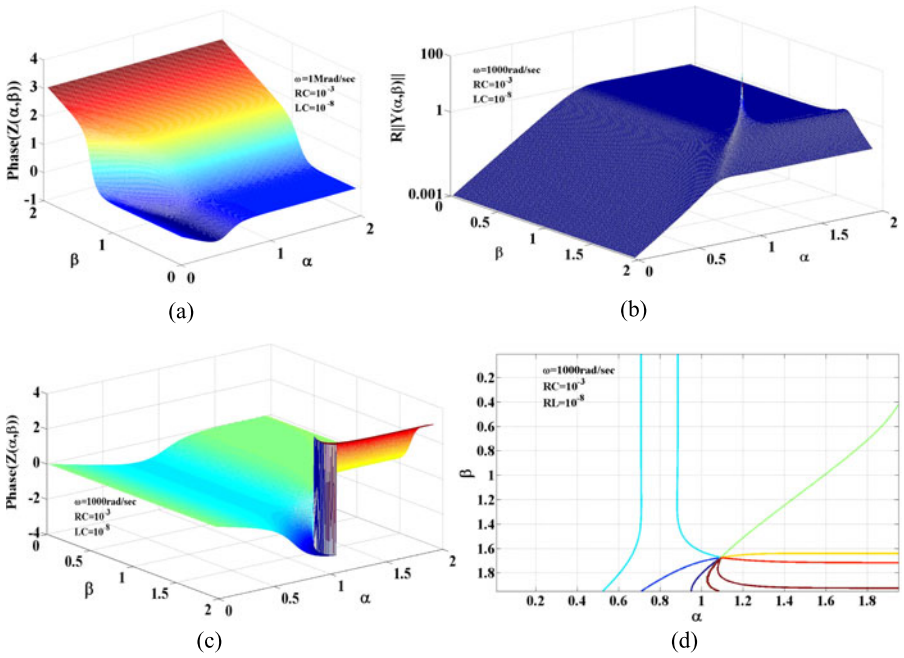**Fig. 10** The admittance magnitude response for different cases with respect to α and β

Fig. 11 (**a**) Phase response versus fractional orders α and β at $\omega = 1$ Mrad/sec, (**b**) admittance magnitude with respect to α and β, (**c**) phase response versus fractional orders α and β at $\omega = 1$ krad/sec, (**d**) the contour of the phase surface at $\omega = 1$ krad/sec

4.2 Sensitivity Analysis of the Magnitude Response

4.2.1 The Effect of (RC)

The magnitude response versus RC has a critical value at $\partial(\|Z(RC)\|/R)/\partial(RC) = 0$. This critical value $(RC)_c$ is given by

$$(RC)_c^{-1} = -\omega^\alpha\left(\omega^\beta\left(\frac{L}{R}\right)\cos\left(\frac{(\alpha+\beta)\pi}{2}\right) + \cos\left(\frac{\alpha\pi}{2}\right)\right) \qquad (15a)$$

At the critical value of RC, the magnitude of this impedance is always minimum and is given by

$$\left(\frac{(\|Z(RC)\|)}{R}\right)_{(RC)_c} = \left|\sin\left(\frac{\alpha\pi}{2}\right) + \omega^\beta\left(\frac{L}{R}\right)\sin\left(\frac{(\alpha+\beta)\pi}{2}\right)\right| \qquad (15b)$$

This minimum value can be zero (short circuit free oscillation) if $(RC)_{\text{sc}}$ is chosen to be $(RC)_c$ and (L/R) is chosen such that $(L/R)_{\text{sc}} = -\sin(\alpha\pi/2)/(\omega^\beta\sin((\alpha+\beta)\pi/2))$. Figure 12(a) shows the values of $(RC)_c$ versus β for different values of the fractional order α at angular frequency $\omega = 1$ Mrad/sec and $R/L = 10^{-6}$. Some curves are plotted for certain ranges of β at which $(RC)_c$ is positive. The magnitude of the admittance versus (RC) is shown in Fig. 12(b) at the listed data. The minimum magnitude of the impedance at $(RC)_c$ is shown in Fig. 12(c), where some local maximum exists for each curve at β_*, and where $\beta_* + \alpha = 1 - (2/\pi)\tan^{-1}(\pi/(2\ln(\omega))) + \text{sgn}(\omega - 1)$. Then if $\omega = 1$ Mrad/sec, $\beta_* + \alpha = 1.9279$ as shown in Fig. 12(c).

4.2.2 The Effect of (L/R)

Similarly, the effect of the parameter (L/R) on the magnitude response is discussed, where the critical value is

$$\left(\frac{L}{R}\right)_c = -\left(\frac{\cos(\frac{(\alpha+\beta)\pi}{2})}{\omega^{\alpha+\beta}RC} - \frac{\cos(\frac{\beta\pi}{2})}{\omega^\beta}\right) \qquad (16a)$$

and the magnitude at the critical value of L/R is given by

$$\left(\frac{(\|Z(RC)\|)}{R}\right)_{(\frac{L}{C})_c} = \left|\sin\left(\frac{\beta\pi}{2}\right) + \frac{\sin(\frac{(\alpha+\beta)\pi}{2})}{\omega^\alpha RC}\right| \qquad (16b)$$

as shown in Fig. 12(d) at $\alpha = 0.5$, $RC = 0.001$, and for different values of operating angular frequency $\omega = \{10^2, 10^4, 10^6\}$ rad/sec. When the operating frequency increases, the critical value decreases. Also, each magnitude response has a minimum value at certain values of β, and this value increases quickly as α increases. The minima of $((\|Z(RC)\|)/R)_{(L/C)_c}$ are not equal as shown; as the frequency increases, the possibility of the short circuit free oscillation case occurring is increased.
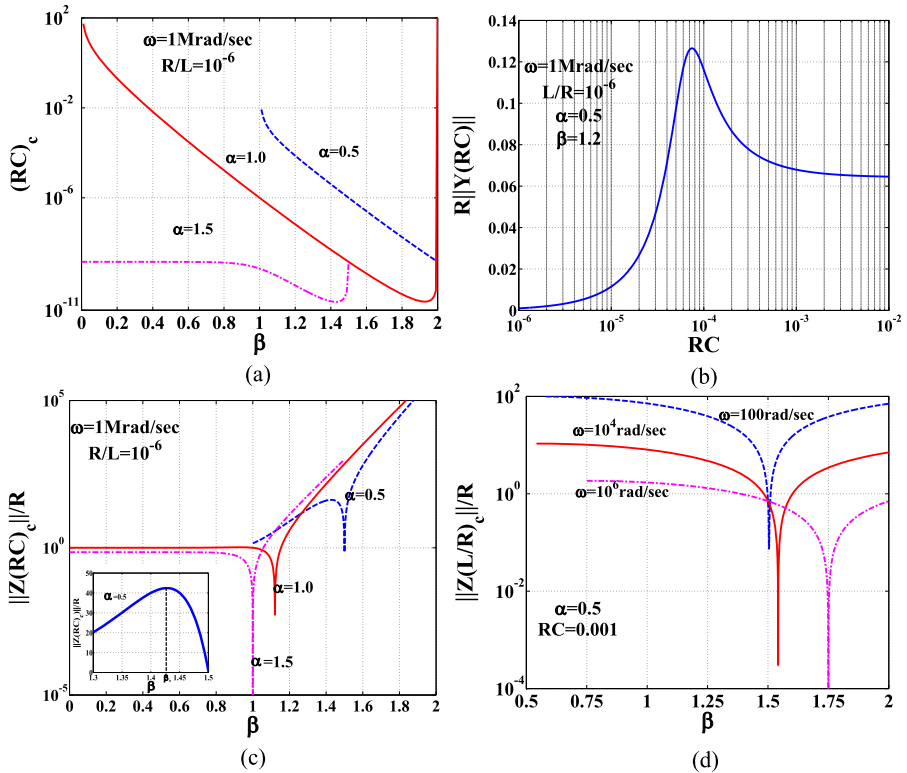
Fig. 12 (**a**) The critical value of RC versus β for different α, (**b**) the admittance magnitude versus RC, (**c**) the impedance magnitude at critical RC versus β for different α, (**d**) the impedance magnitude at critical RC versus β for different ω

4.2.3 The Effect of α, and β

Now, the effect of a small perturbation in each fractional order is discussed separately. Figure 13(a) shows that for $\omega = 1$ Mrad/sec, a small change of 0.1 around the integer order in the fractional order β can be the reason for the magnitude scaling of 100. Moreover, the peak of the admittance magnitude can be highly magnified for a small perturbation as shown in Fig. 13(b) where $\omega = 1000$ rad/sec. When $\alpha = \beta$ the magnitude response will be symmetric around $\omega_o = (LC)^{-1/2\alpha}$ as shown in Fig. 13(c). The magnitude has the same shape and same symmetry axis, but the bandwidth and peaks vary as (RC) changes. However, when $\alpha \neq \beta$ this symmetry is volatile as shown in Fig. 13(d); the lower frequency band is affected with α more than β and vice versa.

5 Optimization Design Examples

Many curves cannot be obtained using the traditional systems, but they may be achieved using the generalized system due to the extra degree of freedom. For example, let us try to model a certain frequency response of a given system by its equiva-
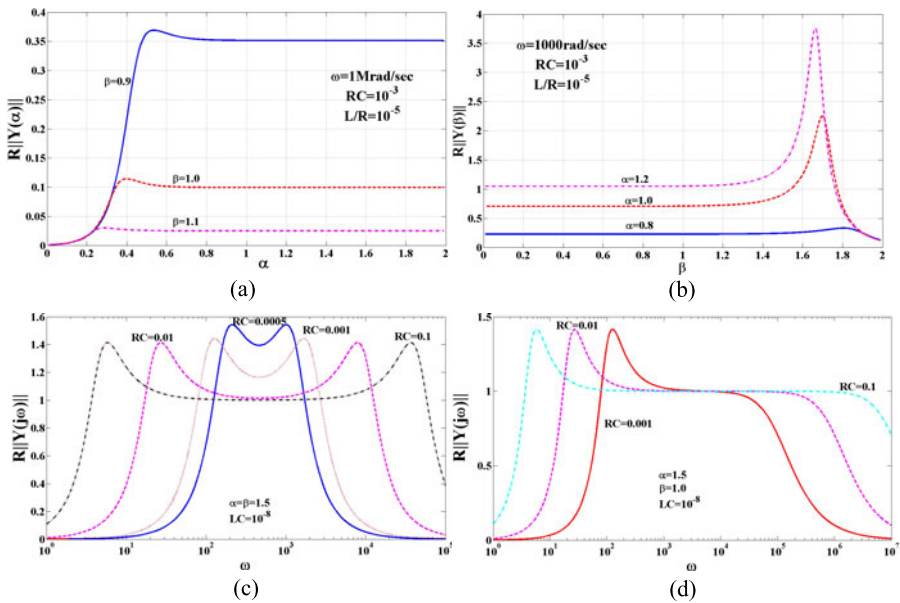
Fig. 13 (**a**) The admittance magnitude versus α for different β, (**b**) the admittance magnitude versus β for different α, (**c**) the admittance magnitude versus frequency for different RC at $\alpha = \beta = 1.5$, (**d**) the admittance magnitude versus frequency for different RC at $\alpha = 1.5$ and $\beta = 1$

lent electrical impedance. Assume the target magnitude response is $R\|Y(j\omega)\|$ of the series connection of $RL_\beta C_\alpha$, with given $RC = 10^{-3}$, $L/R = 10^{-5}$, and unknown fractional order vector $p = (\alpha, \beta)$. Each response has different characteristic issues, like the locations of maxima and minima and their magnitude levels, depending on the vector p. In order to get the best fractional-order vector p for ultimate matching in the frequency range $\omega \in [1, 10^9]$ rad/sec, an appropriate optimization technique is applied to minimize the error between the target and design responses. Fminimax is a very common optimization function used in the Matlab toolbox; it minimizes the maximum absolute error vector between the design and the target responses for all values of ω which belong to its full range. The final optimizer vector p^* is given by

$$P^* = \min_{P \in [\alpha, \beta]} \max_\omega \|Y(j\omega, P) - Y_{\text{tar}}(j\omega)\|, \quad \forall \omega \in [1, 10^9] \qquad (17)$$

The optimization initial factors are given as $P_{\min} = [0.1, 0.1]$, $P_{\max} = [1.9, 1.9]$, and the initial value chosen for the fractional-order vector is $P_o = [1.0, 1.0]$, which is the known traditional integer-order case. The previous example can be extended for more orders, as seen in the next example, where the target fractional orders are given by $\alpha = 1.3$, and $\beta = 1.4$. The target response is shown in Fig. 14, where one can see that this response has different characteristics than the traditional RLC like two unequally local maxima points and one minimum point.

Using the same previous initializations, Table 1 shows the relation between the number of iterations, output optimizer fractional order $p = [\alpha, \beta]$, and the maximum absolute error, which is given by $\max_\omega \|Y(j\omega, \alpha, \beta) - Y_{\text{tar}}(j\omega)\|$, $\forall \omega \in [1, 10^6]$. The

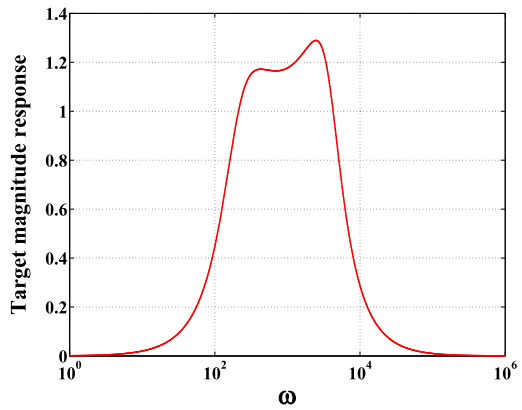**Fig. 14** The target response of the series $RL_\beta C_\alpha$

Table 1 Maximum absolute error versus number of iterations

N	α	β	Maximum absolute error
1	1	1	0.910567211818491
10	1.04227314691733	1.19058231285022	0.783363021308538
20	1.04227314691733	1.19058233059128	0.783363021223020
30	1.04490638447112	1.18898520365004	0.778424042483930
40	1.06022855723747	1.20830274920557	0.748398459660243
50	1.25219002840919	1.43482334357574	0.194130776067777
60	1.25184892989467	1.43459027754894	0.192758239858582
70	1.25188107461205	1.43396172513362	0.189144232680705
80	1.25430797421031	1.43233954829452	0.180024413899684
90	1.27241094543248	1.41993080005695	0.110599232446168
100	1.28687148026980	1.40966695797841	0.0533604622831690
110	1.30000000146210	1.39999984153281	8.84091893582628e-07
118	1.29999999999992	1.40000000000941	5.24729149020686e-11

maximum error decreases from 0.91056 to 5.247×10^{-11} in 118 iterations, and the fractional orders adapt themselves gradually, as shown in the table. The fractional order β changes from 1.0, then increases to more than 1.43, and finally return back to 1.4, which demonstrates the oscillations which can happen in order to reach their optimized values.

Figure 15(a) shows five responses at different iterations at $N = 1, 20, 60, 90$, and 118, which are shown in the first column in Table 1; the second and third columns are the optimized fractional orders. As seen, the responses try to capture the main characteristics of target response. When $N = 1$ (integer case) the response is flat with a single maximum and wide spectrum; then at $N = 20$, the response changes the location of the maximum and its width; after 50 iterations, the response is almost in the same band of frequencies and tries to improve to be closer to the target response. The maximum absolute error exponentially decreases with the number of iterations as shown in Fig. 15(b).

Fig. 15 (**a**) The response for five different iterations, (**b**) the maximum absolute error versus the number of iterations, (**c**) the optimizer output and the target orders for 42 different target cases
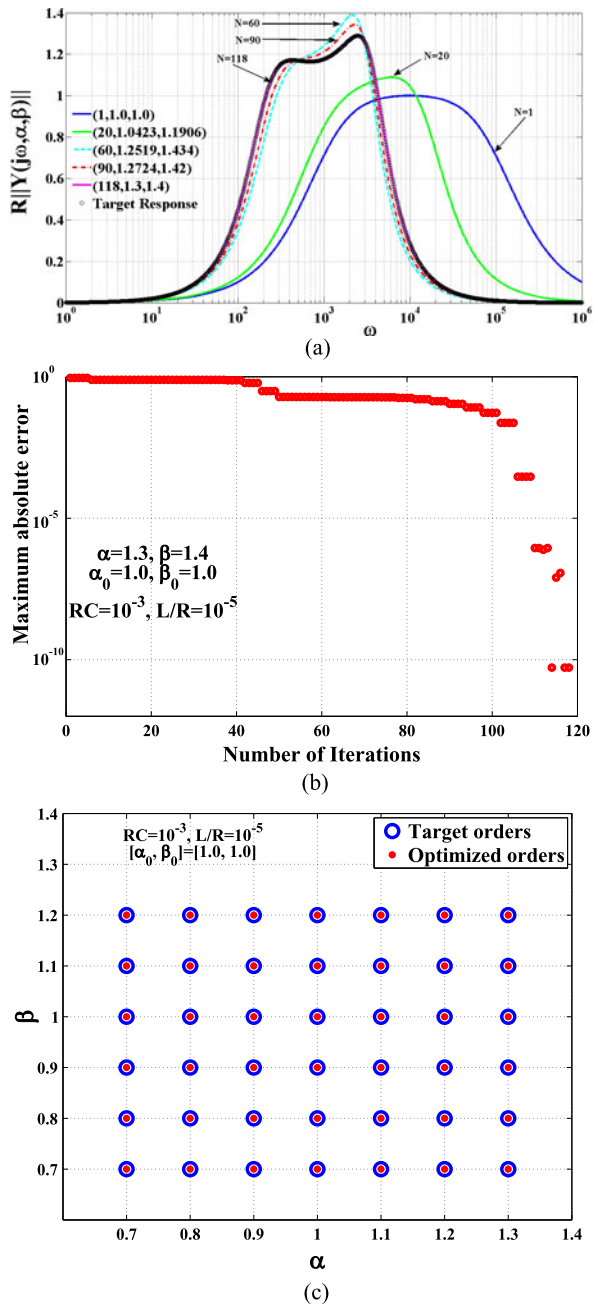

Figure 15(c) shows the final output optimizer vector and the target fractional-order vector for different values of α and β using the analytical derivatives of the designed response. More than 40 cases are tested during this example, illustrating excellent fractional-order detection.

6 Conclusion

This paper discussed the effects of using fractional-order elements (fractional-order capacitor and fractional-order inductor) instead of integer-order elements in series *RLC* circuits where new fundamentals and generalizations of the known fundamentals in circuit theory are introduced, such as generalized expressions for pure resistive, pure inductive, and pure capacitive conditions. Furthermore, the introduction of free oscillation conditions is derived. Sensitivity analyses of all circuit parameters are introduced given closed-form expressions to be used in the gradient-based optimization for filter design, where more than 40 different design examples are tested, showing a perfect response detection.

References

1. K. Biswas, S. Sen, P. Dutta, Modelling of a capacitive probe in a polarizable medium. Sens. Actuators Phys. **120**(1), 115–122 (2005)
2. G. Carlson, C. Halijak, Approximation of fractional capacitors $(1/s)^{1/n}$ by a regular Newton process. IEEE Trans. Circuit Theory **11**(2), 210–213 (1964)
3. K. Diethelm, N.J. Ford, A.D. Freed, Y.Y. Luchko, Algorithms for the fractional calculus: a selection of numerical methods. Comput. Methods Appl. Mech. Eng. **194**(6), 743–773 (2005)
4. T.C. Doehring, A.H. Freed, E.O. Carew, I. Vesely, Fractional order viscoelasticity of the aortic valve: an alternative to QLV. J. Biomech. Eng. **127**(4), 700–708 (2005)
5. A.S. Elwakil, B. Maundy, Extracting the Cole-Cole impedance model parameters without direct impedance measurement. Electron. Lett. **46**(20), 1367–1368 (2010)
6. M. Faryad, Q.A. Naqvi, Fractional rectangular waveguide. Prog. Electromagn. Res. **75**, 384–396 (2007)
7. N.J. Ford, A.C. Simpson, The numerical solution of fractional differential equations: speed versus accuracy. Numer. Algorithms **26**(4), 333–346 (2001)
8. M.E. Fouda, A.G. Radwan, On the fractional-order memristor model. J. Fract. Calc. Appl. **4**(1), 1–7 (2013)
9. T.C. Haba, G.L. Loum, J.T. Zoueu, G. Albart, Use of a component with fractional impedance in the realization of an analogical regulator of order ½. J. Appl. Sci. **8**(1), 59–67 (2008)
10. T.C. Haba, G.L. Loum, G. Ablart, An analytical expression for the input impedance of a fractal tree obtained by a microelectronical process and experimental measurements of its non-integral dimension. Chaos Solitons Fractals **33**(2), 364–373 (2007)
11. T.C. Haba, G. Ablart, T. Camps, F. Olivie, Influence of the electrical parameters on the input impedance of a fractal structure realised on silicon. Chaos Solitons Fractals **24**(2), 479–490 (2005)
12. I.S. Jesus, J.A. Machado, J.B. Cunha, M.F. Silva, Fractional order electrical impedance of fruits and vegetables, in *Proceedings of the 25th IASTED International Conference on Modeling Identification and Control* (2006), pp. 489–494
13. I.S. Jesus, J.A. Machado, Development of fractional order capacitors based on electrolyte processes. Nonlinear Dyn. **56**(1), 45–55 (2009)
14. B.T. Krishna, Studies on fractional order differentiators and integrators: a survey. Signal Process. **91**(3), 386–426 (2011)
15. B.T. Krishna, K.V.V.S. Reddy, Active and Passive Realization of Fractance Device of Order 1/2. Act. Passive Electron. Compon. **2008** (2008)
16. H. Li, M. Wu, X. Wang, Fractional-moment capital asset pricing model. Chaos Solitons Fractals **42**(1), 412–421 (2009)
17. R.L. Magin, Fractional calculus in bioengineering. Begell House, Connecticut (2006)
18. R.L. Magin, Fractional calculus in bioengineering, part 3. Crit. Rev. Biomed. Eng. **32**(3–4), 195–377 (2004)
19. R.L. Magin, M. Ovadia, Modeling the cardiac tissue electrode interface using fractional calculus. J. Vib. Control **14**(9–10), 1431–1442 (2008)

20. R. Martin, J.J. Quintara, A. Ramos, L. Nuez, Modeling electrochemical double layer capacitor, from classical to fractional impedance, in *Proceedings of the 14th IEEE Mediterranean Electrotechnical Conference* (2008), pp. 61–66
21. K.S. Miller, B. Ross, *An Introduction to the Fractional Calculus and Fractional Differential Equations* (Wiley, New York, 1993)
22. K. Moaddy, A.G. Radwan, K.N. Salama, S. Momani, I. Hashim, The fractional-order modeling and synchronization of electrically coupled neuron systems. Comput. Math. Appl. **64**(10), 3329–3339 (2012)
23. M. Nakagawa, K. Sorimachi, Basic characteristics of a fractance device. IEICE Trans. Fundam. Electron. Commun. Comput. Sci. **E75-A**(12), 1814–1819 (1992)
24. K.B. Oldham, J. Spanier, *Fractional Calculus* (Academic Press, New York, 1974)
25. I. Petras, D. Sierociuk, I. Podlubny, Identification of parameters of a half-order system. IEEE Trans. Signal Process. **60**(10), 5561–5566 (2012)
26. I. Petras, Y. Chen, Fractional-order circuit elements with memory, in *Proceedings of the 13th International Carpathian Control Conference* (2012), pp. 552–558
27. I. Petras, *Fractional-Order Nonlinear Systems: Modelling, Analysis and Simulation* (Springer, Berlin, 2011)
28. A.G. Radwan, A.S. Elwakil, A.M. Soliman, Fractional-order sinusoidal oscillators: design procedure and practical examples. IEEE Trans. Circuits. Syst., I **55**(7), 2051–2063 (2008)
29. A.G. Radwan, A.M. Soliman, A.S. Elwakil, Fractional-order sinusoidal oscillators: four practical circuit design examples. Int. J. Circuit Theory Appl. **36**(4), 473–492 (2008)
30. A.G. Radwan, A.M. Soliman, A.S. Elwakil, First order filters generalized to the fractional domain. J. Circuits Syst. Comput. **17**(1), 55–66 (2008)
31. A.G. Radwan, A.S. Elwakil, A.M. Soliman, On the generalization of second-order filters to fractional-order domain. J. Circuits Syst. Comput. **18**(2), 361–386 (2009)
32. A.G. Radwan, K.N. Salama, Fractional-order RC and RL circuits. Circuits Syst. Signal Process. **31**(6), 1901–1915 (2012)
33. A.G. Radwan, K.N. Salama, Passive and active elements using fractional $L_\beta C_\alpha$ circuit. IEEE Trans. Circuits Syst. I **58**(10), 2388–2397 (2011)
34. A.G. Radwan, Stability analysis of the fractional-order $RL_\beta C_\alpha$ circuit. J. Fract. Calc. Appl. **3**(1), 1–15 (2012)
35. A.G. Radwan, M.H. Bakr, N.K. Nikolova, Transient adjoint sensitivities for discontinuities with Gaussian material distributions. Prog. Electromagn. Res. B **27**, 1–19 (2011)
36. S. Roy, On the realization of a constant-argument immitance or fractional operator. IEEE Trans. Circuit Theory **14**(3), 264–274 (1967)
37. J. Sabatier, O.P. Agrawal, M.J.A. Tenreiro, *Advances in Fractional Calculus; Theoretical Developments and Applications in Physics and Engineering* (Springer, Berlin, 2007)
38. K. Saito, M. Sugi, Simulation of power-law relaxations by analog circuits: fractal distribution of relaxation times and non-integer exponents. IEICE Trans. Fundam. Electron. Commun. Comput. Sci. **E76**(2), 205–209 (1993)
39. I. Schäfer, K. Krüger, Modelling of lossy coils using fractional derivatives. J. Phys. D, Appl. Phys. **41**(4), 045001 (2008)
40. A. Soltan, A.G. Radwan, A.M. Soliman, Fractional order filter with two fractional elements of dependent orders. J. Microelectron. **7**(9), 965–969 (2012)
41. M. Sugi, Y. Hirano, Y.F. Miura, K. Saito, Simulation of fractal immitance by analog circuits: an approach to the optimized circuits. IEICE Trans. Fundam. Electron. Commun. Comput. Sci. **E82**(8), 1627–1634 (1999)
42. J. Valsa, Fractional-order electrical components, networks and systems, in *Proceedings of the 22nd International Conference Radioelektronika* (2012), pp. 1–9
43. S. Westerlund, L. Ekstam, Capacitor theory. IEEE Trans. Dielectr. Electr. Insul. **1**(5), 826–839 (1994)